



Implementation aspects of the Boundary Element Method including viscous and thermal losses

Vicente CUTANDA HENRIQUEZ¹; Peter JUHL²

^{1,2}University of Southern Denmark, Denmark

ABSTRACT

The implementation of viscous and thermal losses using the Boundary Element Method (BEM) is based on the Kirchhoff's dispersion relation and has been tested in previous work using analytical test cases and comparison with measurements. Numerical methods that can simulate sound fields in fluids including losses are particularly interesting whenever small cavities and narrow passages are present, as is the case with many acoustic devices such as transducers and small audio appliances.

The present paper describes current work aimed at improving the method by addressing some specific issues related with mesh definition, geometrical singularities and treatment of closed cavities. These issues are specific of the BEM with losses. Using examples, some strategies are presented that can alleviate shortcomings and improve performance.

Keywords: Visco-thermal, losses, BEM

I-INCE Classification of Subjects Number(s): 75.5

1. INTRODUCTION

The issue of viscous and thermal losses in small domains has been a matter of attention in the literature in recent years. Lately the implementation of such losses in numerical methods has become a reality and is bringing new understanding of the acoustics of small devices such as microphones, couplers, hearing aids or mobile phones.[1,2]

Theory on losses is based on the Navier-Stokes set of equations where linearity and no flow is assumed, but losses are kept.[3,4] Direct implementation of the equations using the Finite Element Method (FEM) has been proposed and later implemented in a commercial software package.[5,6]

By means of Kirchhoff's dispersion equation it is possible to separate the lossy acoustic sound field into three modal wave fields: viscous, thermal and acoustic.[3,7] These three modes are coupled at the domain boundary. A Boundary Element Method (BEM) implementation makes use of this theoretical framework by calculating the three modes and building the solution through coupling of the viscous and thermal boundary conditions.[8,9,10,11].

This paper examines a few particular aspects of the BEM implementation of losses related with its efficiency, performance and practical use. As an example, an axisymmetrical model of a Brüel & Kjær ¼ inch type 4938 condenser microphone is presented in section 2 and used in the rest of the paper. In section 3, the numerical difficulty of the zero frequency cavity mode arising in BEM is examined and a solution proposed. The meshing of critical parts of the domain boundary, in particular sharp corners is treated in section 4. Section 5 explains some efficiency improvements in the way the BEM handles the viscous and thermal modes.

2. TEST CASE

The B&K 4938 microphone is a pressure-field measurement condenser microphone with no holes in the backplate, therefore suitable for axisymmetrical modeling. Only the internal cavity and the

¹ vch@mmmi.sdu.dk

² pmjuhl@mmmi.sdu.dk

diaphragm are modeled, while the external excitation used is a uniform sound pressure of 1 Pa amplitude acting on the membrane. More complicated models already exist (i.e. three-dimensional, external medium), but this simplification is however sufficient and convenient for the purpose of the paper. The microphone external appearance and the internal geometry are depicted in figure 1.

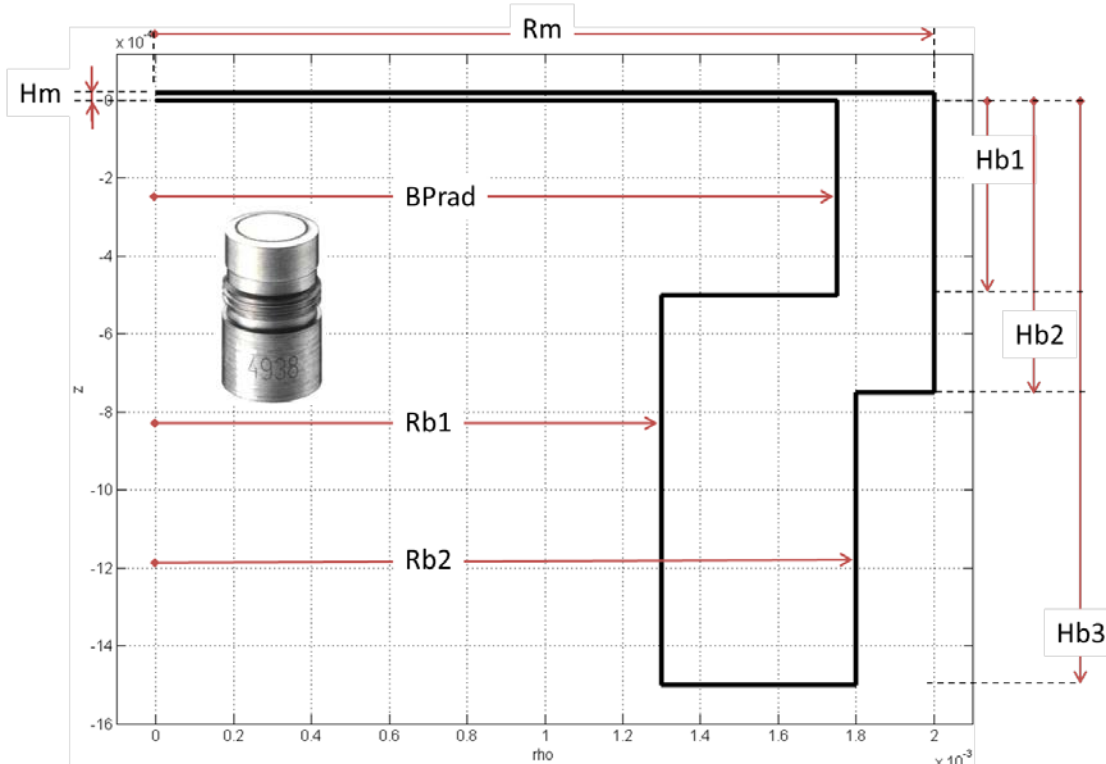


Figure 1 – Appearance and internal geometry generator of the B&K 4938 microphone.

The dimensions are: $R_m = 2$ mm, $H_m = 19.5$ μm , $B_{\text{Prad}} = 1.75$ mm, $R_{b1} = 1.3$ mm, $R_{b2} = 1.8$ mm, $H_{b1} = 0.5$ mm, $H_{b2} = 0.75$ mm, $H_{b3} = 1.5$ mm. The membrane is modeled using one-dimensional FEM, and is coupled to the BEM model with losses of the internal cavity. R_m is the radius of the membrane, which covers the top of the geometry and is fixed at the rim. The membrane tension is 3128 N/m, its density 8300 kg/m³ and the thickness 6,95 μm . The very thin gap (H_m) is where most of the losses occur and act on the membrane as a damping force. The rim of the backplate, of radius B_{Prad} , is the only connection between the gap and the back cavity.

The microphone sensitivity is proportional to the average displacement of the membrane. The sensitivity can be measured under equivalent conditions using an electrostatic actuator, but the manufacturing tolerances give rise an important margin of variation from unit to unit.

3. NUMERICAL DIFFICULTY AT LOW FREQUENCY

The direct collocation BEM implementation used in the calculations poses a difficulty when dealing with hard-walled closed interior domains. Such cavities have an eigenmode at zero frequency along with the eigenmodes dictated by the cavity's geometry and dimensions. In BEM, the calculation at frequencies close to eigenmodes shows as a high condition number of the coefficient matrix associated with node pressures, the \mathbf{A} matrix following the notation in reference [11]. See also reference [12] for a practical use of the condition numbers of BEM coefficient matrices.

Figure 2 shows the sensitivity of the microphone calculated with a totally hard interior boundary. It is compared with a result where one of the backcavity nodes is given a non-zero (0.005) admittance. The existence of some admittance moderates the condition number of the coefficient matrix at low frequency and allows a meaningful solution to be obtained.

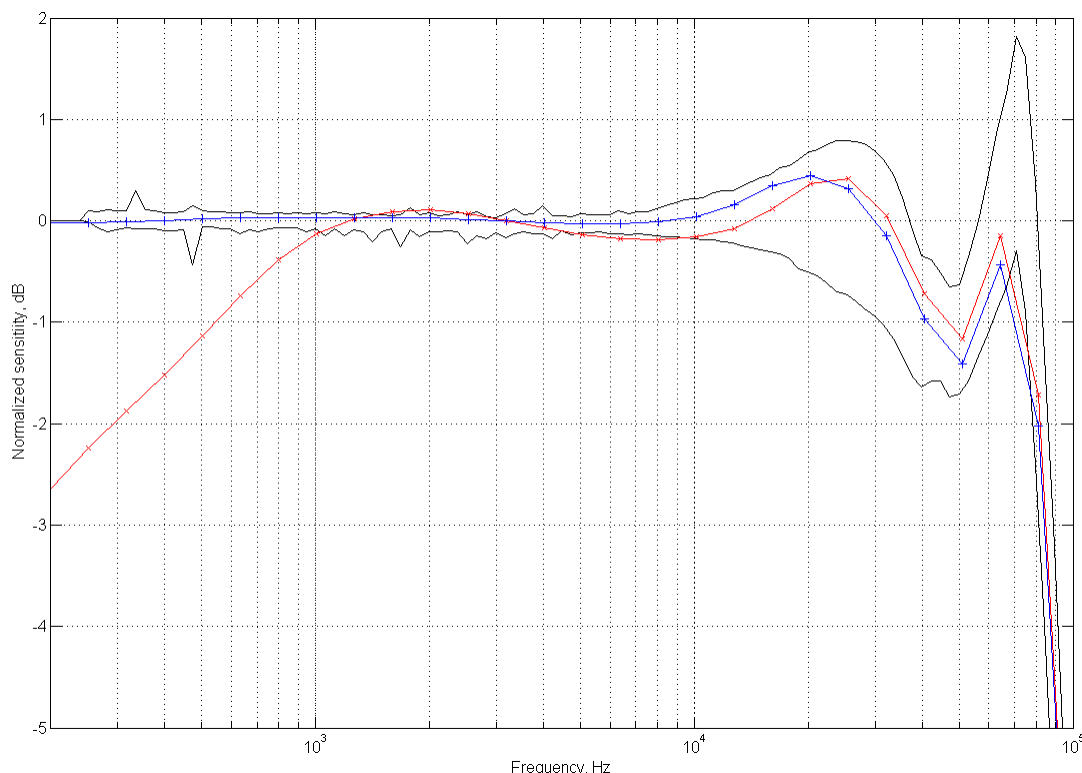


Figure 2 –Normalized sensitivity of the B&K 4938 microphone. Black curves, higher and lower limits of a large set of actuator measurements; red “x”, BEM result with hard-walled back cavity; blue “+”, BEM result with one node in the back cavity with non-zero admittance.

Figure 3 shows the condition numbers of the **A** coefficient matrix in a sphere with a 2 mm radius (the same as the B&K 4938 example) and 20 generator elements. The high condition number indicates that the solution is more sensitive to small variations of pressure and velocity on the boundary, but it does not usually prevent correctly solving in the lossless case. However, in complicated setups with coupling and losses, as is the case of the B&K 4938 microphone, there are further approximations, more variables and therefore machine errors build up; the effect can trigger calculation errors at low frequencies.

A remedy can be the introduction of some small impedance somewhere on the setup boundary. This would reduce the effect of the $f=0$ eigenmode and render more stable calculations. Figure 3 also includes a condition number curve plot where one of the nodes on the sphere’s interior is given an acoustic admittance of 0.005; the coefficient matrix becomes then $\mathbf{A}+ikZ_0\mathbf{B}\mathbf{Y}$, with **B** the coefficient matrix associated with normal velocity, k the wavenumber, Z_0 the characteristic impedance of air and **Y** the boundary admittances, following again reference [11].

Figure 4 shows the effect on the calculation of the internal pressure in the spherical cavity, if it is excited by a moving cap of 20 degrees radius at the top, and calculated at the opposite side of the cavity. The calculation and impedance points are indicated with ‘*’ at the bottom and side respectively of the sketch in figure 4.

The theoretical lumped parameter pressure in the sphere can be calculated as the product of the volume velocity of the moving cap (normal velocity times the area) times the acoustic impedance of the sphere ($\rho c/i\omega V$). It is plotted in figure 4 as well.

Introducing non-zero admittance obviously changes the setup to some degree, as can be seen in the sphere case in figure 4. In the B&K microphone modeled in this paper, the prescribed admittance on one backcavity node helps achieving a meaningful result, without significantly modifying the expected sensitivity result.

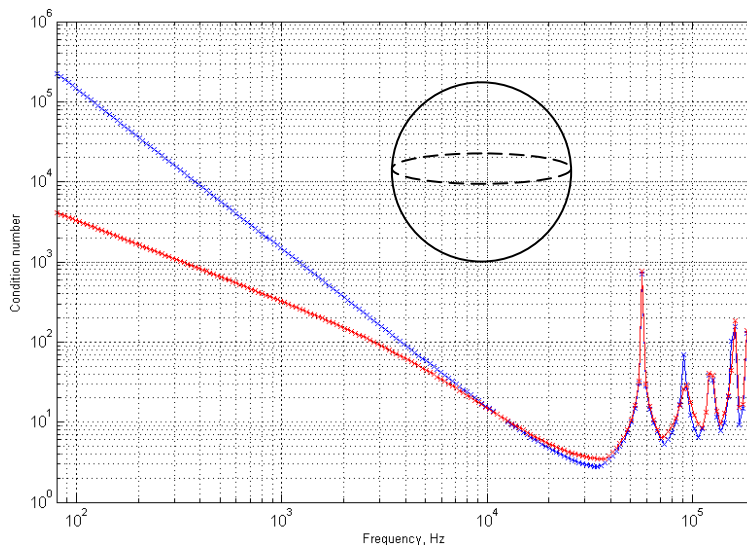


Figure 3 – Calculations on a hollow sphere. Condition numbers of the A coefficient matrix with hard boundary (blue) and one node with non-zero admittance (red).

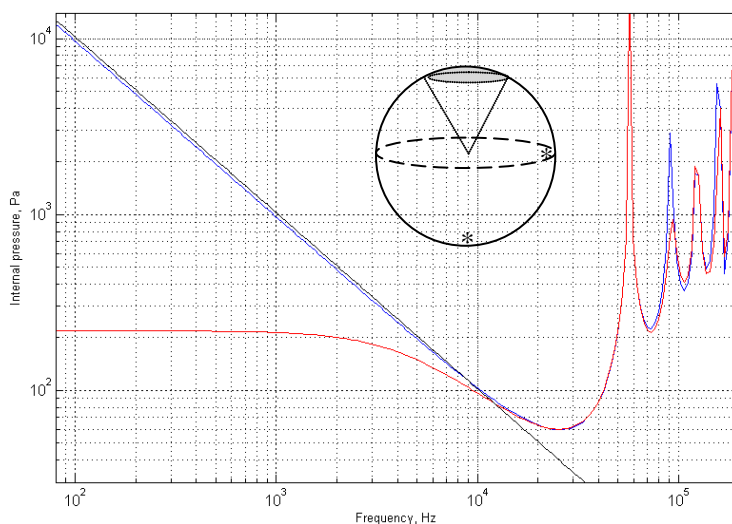


Figure 4 – Calculations on a hollow sphere. Pressure magnitude at the interior: black, lumped parameter result; blue, hard boundary; and red, one node with non-zero admittance.

4. MODELING OF THE SHARP CORNER AT THE RIM

In lossless BEM, the mesh density is usually set to have a minimum of six nodes per wavelength. This rule of thumb ensures that sound field variations can be followed, since those variations will occur within shorter distances, the higher the frequency.

Viscous and thermal losses have a short range away from the boundaries and can be considered as diffusion processes combined with wave propagation. The effects are local and depend mostly on the local boundary shape. Both in lossy and lossless models, sharp corners are geometrical singularities that cause significant variations of the sound field in their vicinity, posing a modeling challenge. [13,14]

Considering losses means an extra constraint on the boundary shape: the surface must be C^1 differentiable.[7] In the BEM with losses, the non-slip condition for the viscosity mode is implemented using a second tangential derivative. A sharp corner is therefore a violation of the theory

of losses on which the numerical models are based. Even with no losses, the corner results in a discontinuity of the normal velocity. Some authors offer remedies for this situation, but only in the lossless case. [15,16]

In lossless acoustics, corner effects are usually ignored with no significant consequences. There are however cases where losses must be considered and where the behavior near a corner does affect the overall result. The example in this paper is one of such cases. It contains a number of sharp corners, but the calculations show that the sound field near the corner situated at the rim of the backplate ($\rho=1.75$, $z=0$ in figure 1) has an influence on the overall performance and must be properly modeled. Figure 5 shows the particle velocity in the region around this corner, calculated using the BEM with losses. These are instantaneous values; the velocity vectors change direction and magnitude during a wave period.

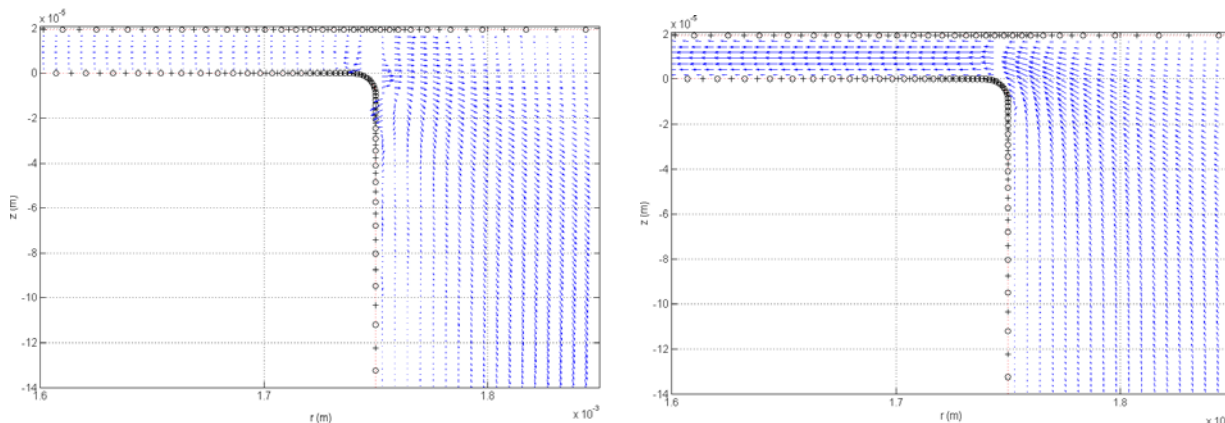


Figure 5 – Particle velocity around the backplate rim corner of the B&K 4938 microphone. Left, 0 deg. phase; right, 90 deg. phase.

The modeling of a corner can be dealt with by a local increase of mesh density. This is usually done in FEM with losses. In BEM, the corner can be finished with a curved boundary section with a short curvature radius. The corner has been rounded in the case of figure 5; other curvature radii and mesh densities have been tried, showing that the meshing effort can be concentrated to the region on the corner and its immediate vicinity. The rest of the mesh can be meshed with a much rougher mesh. In the limit of zero curvature, the corner will tend towards a geometrical singularity.

Figures 6 and 7 show the meshed generators and the sensitivity results for the B&K 4938 microphone calculated with a sharp corner and with a rounded corner with extra elements; the differences are obvious. The mesh with rounded corner has 111 elements and 223 nodes, while the regular mesh has 135 elements and 271 nodes, that is, the best result is actually obtained with less elements and nodes, but concentrated on the troublesome area.

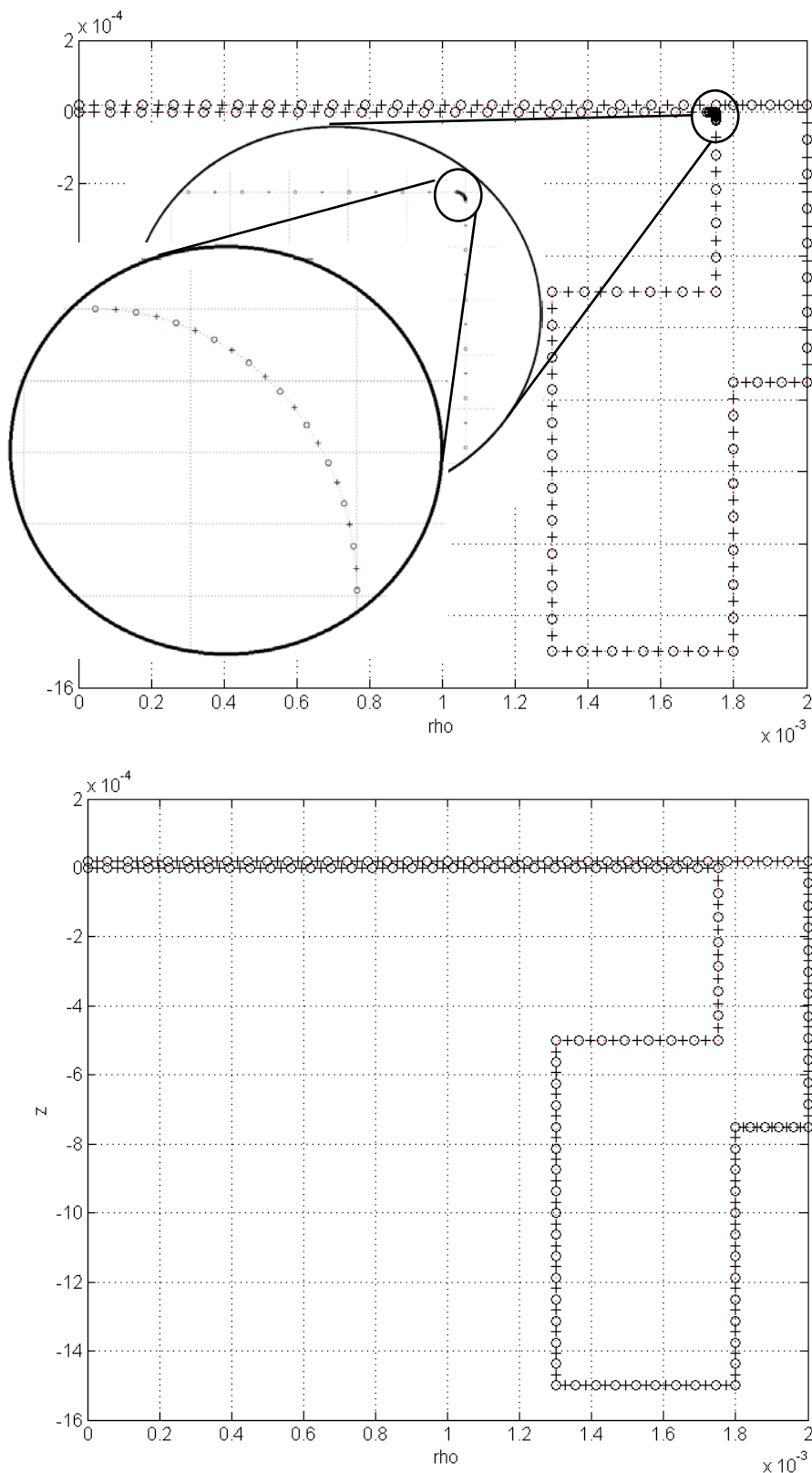


Figure 6 –Two BEM generator meshes of the B&K 4938 microphone. Upper plot, mesh with rounded rim corner, 111 quadratic elements; lower plot, mesh with no rounding, 135 quadratic elements.

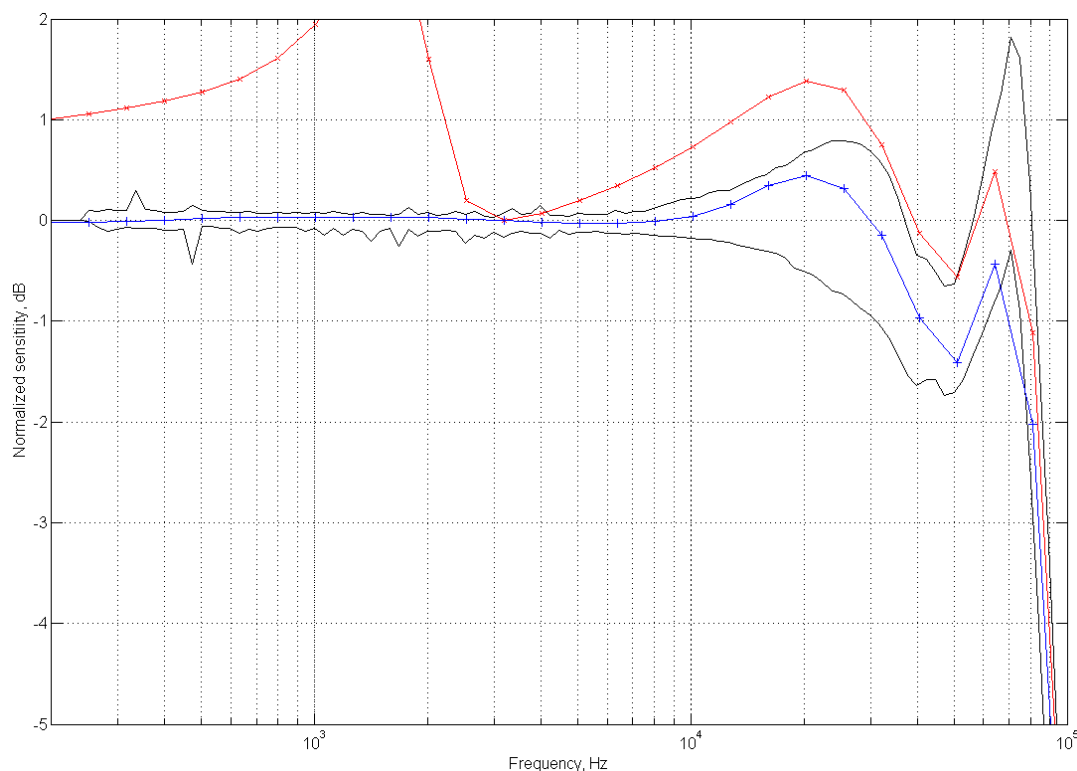


Figure 7 –Sensitivity of the B&K 4938 microphone. Red ‘x’, sharp rim corner; blue ‘+’, smoothed rim corner. The meshes used are those of figure 6.

5. EFFICIENCY IMPROVEMENTS

The BEM coefficient matrices contain integrals of two kernels that essentially (that is, besides element shape functions and the jacobian of the transformation from global to local coordinates) contain the Green’s function $G(R)=\exp(-jkR)/(4\pi R)$ and its normal derivative $\partial G(R)/\partial n$. Here R is the distance from the running integration point to the collocation point. In an axisymmetric implementation the surface integral is carried out as an integral along the generator combined with a circumferential integral.[8]

To speed up calculations, two improvements of the implementation can be made:

- Firstly, it is not necessary to model the small gap between the diaphragm and the backplate using elements that are comparable with the gap thickness. Much larger elements can be used if the near singular behavior is dealt with using a local refinement of the numerical integration – rather than a refinement of the mesh.[17]
- Secondly, viscous and thermal modes are calculated with formally the same kernel as in the lossless case, but using complex wavenumbers. The imaginary part of the complex wavenumber leads to an exponential decay reflecting the fact that the viscous and thermal modes are local, as opposed to the acoustic mode, which is global. Hence, a simple check of the distance between the element and the collocation point can be carried out initially and used to avoid calculating contributions that are efficiently zero due to the exponential decay.

For collocation points close to the element, the integral refinement ensures that both the near-singularity and the fast variation of the exponential decay are handled accurately and efficiently.

6. CONCLUSIONS

Several implementation issues concerning the use of the BEM in acoustics with viscous and thermal losses have been examined in this paper. A particularly challenging test case has been used as an example when dealing with such issues, the Brüel & Kjær microphone type 4938.

The effect of a totally rigid interior cavity gives rise to errors in the calculation at low frequencies. This effect is reduced by introducing some impedance in the microphone's back cavity, rendering meaningful results.

The special treatment of particularly sensitive areas of the setup, where losses and geometrical singularities are present, with finer meshes and rounded corners can give good results with no overall increase of degrees of freedom.

The efficiency of the calculation can be greatly improved by considering details such as the treatment of near-singular kernels and complex wavenumbers.

REFERENCES

1. Homentcovschi D. and Miles R. N. An analytical-numerical method for determining the mechanical response of a condenser microphone, *Journal of the Acoustical Society of America* 2011 130 (6), 3698–3705.
2. Christensen R., Juhl P. and Cutanda Henriquez V. Practical modeling of acoustic losses in air due to heat conduction and viscosity. *Acoustics 08 Paris (Acoustica Society of America and European Acoustics Association)*. 29 June to 4 July 2008 Paris, France. pp. 3269-3274.
3. Pierce A. D. *Acoustics - An Introduction to Its Physical Principles and Applications*. Acoustical Society of America, New York, 1989.
4. Temkin S. *Elements of Acoustics* (Wiley, New York, 1981), Sec. 6.9, pp.434–445.
5. Kampinga R. An efficient finite element model for viscothermal acoustics. *Acta Acust. Acust.* 97, 618–631 (2011).
6. Malinen M., Lyly M., Råback P., Kärkkäinen A. and Kärkkäinen L. A finite element method for the modeling of thermo-viscous effects in acoustics. *Proceedings of the 4th European Congress Computational Methods in Applied Sciences and Engineering ECCOMAS*, Jyväskylä, Finland 2004. pp. 1–12.
7. Bruneau M., Herzog Ph., Kergomard J. and Polack J. D. General formulation of the dispersion equation in bounded visco-thermal fluid, and application to some simple geometries. *Wave Motion* 11, 441–451 (1989).
8. Cutanda Henriquez V., Juhl P. M. An axisymmetric boundary element formulation of sound wave propagation in fluids including viscous and thermal losses. *Journal of the Acoustical Society of America*, 2013, 134(5):3409-3418.
9. Cutanda Henriquez V., Juhl P. M. Implementation of an Acoustic 3D BEM with Visco-Thermal Losses. *Internoise 2013*; 15-18 Sept, 2013; Innsbruck (Austria).
10. Juhl P. M., Cutanda Henriquez V. Verification of an Acoustic 3D BEM with Visco-Thermal Losses. *Internoise 2013*; 15-18 Sept, 2013; Innsbruck (Austria).
11. Cutanda Henriquez V., Juhl P. M. OpenBEM - An open source Boundary Element Method software in Acoustics. In *Proceedings of Internoise 2010*; 13-16 June 2010; Lisbon, Portugal.
12. Olsen E.S., Cutanda Henriquez V., Gramtorp J. and Eriksen A. Calculating the Sound Field in an Acoustic Intensity Probe Calibrator – A Practical Utilization of Boundary Element Modelling. *Proceedings of Eighth International Congress on Sound and Vibration*, 2-6 July 201; Hong Kong, China, pp. 2313-2321.
13. Juhl P. A note on the convergence of the direct collocation boundary element method. *Journal of Sound and Vibration*, 1998 Vol. 212 (4), pp.703-719.
14. Teeby B.E. and Pan J. A practical examination of the errors arising in the direct collocation boundary element method for acoustic scattering. *Engineering Analysis with Boundary Elements* 33 (2009), 1302-1315.
15. Marin L., Lesnic D., Mantič V. Treatment of singularities in Helmholtz-type equations using the boundary element method. *Journal of Sound and Vibration* 278 (2004), 39–62.
16. Ji Lin, Wen Chen and Chen C.S. Numerical treatment of acoustic problems with boundary singularities by the singular boundary method 333 (2014), 3177–3188.
17. Cutanda Henriquez V., Juhl P. and Jacobsen F. On the modeling of narrow gaps using the standard boundary element method, *J. Acoust. Soc. Am.* 109, 1296–1303 (2001).